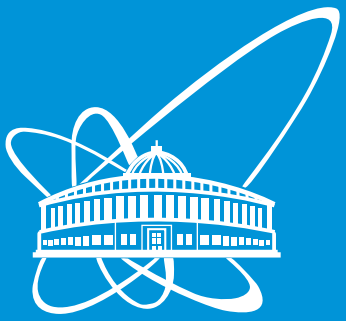

ОБЪЕДИНЕННЫЙ
ИНСТИТУТ
ЯДЕРНЫХ
ИССЛЕДОВАНИЙ

Дубна

E4-2000-103

V.K.Lukyanov, B.Słowinski*, E.V.Zemlyanaya

# ON THE ROLE OF NUCLEAR SURFACE IN HEAVY ION REACTION CROSS SECTION FORMATION

Submitted to «Ядерная физика»

*Faculty of Physics, Warsaw University of Technology, Warsaw, Poland;
Institute of Atomic Energy, Otwock-Swierk, Poland

2000

# 1 Introduction

It is of interest to investigate total reaction cross sections at energies from tens of MeV to 1 GeV per nucleon in view of studying the heavy-ion reaction mechanism and important practical tasks, for example, the problem of transmutation of radioactive waste (see [1]). At intermediate energies when $E \gg U$, $kR \gg 1$, the reaction cross section can be calculated within the Glauber-Sitenko approach [2], [3] accounting to which

$$\sigma_R = 2\pi \int_0^\infty db\, b\, (1 - e^{-2Im\ \Phi_N}), \tag{1.1}$$

where $b$ is the impact parameter, and the nuclear component of total eikonal phase $\Phi_N$

$$\Phi(b) = -\frac{1}{\hbar v} \int_{-\infty}^{\infty} dz\ U(\sqrt{b^2 + z^2}) = -\frac{U_0}{\hbar v} I(b) \tag{1.2}$$

is expressed through the profile integral

$$I(b) = \int_{-\infty}^{\infty} dz\ u(\sqrt{b^2 + z^2}). \tag{1.3}$$

Here $u(b)$ is the distribution function of a potential, and the path integration is performed along the axis $z$ directed as the momentum $\vec{k}_i$ of a projectile nucleus.

Nucleus-nucleus optical potentials are obtained, in general, as a result of a fit to experimental data of the elastic scattering differential cross sections and total cross sections at a given collision energy. Their dependence on energy can be determined if one calculates the phase $\Phi(b)$ in the multiple diffraction scattering method where $\Phi_N$ is expressed by the total nucleon- nucleon cross section whose E-dependence is known. Within such an approximation, the phase is constructed as the convolution of the density distribution functions of nucleons in the projectile $\rho_p$ and target nucleus $\rho_t$. Thus, ultimate calculations of integrals like (1.3) are necessary, too, but with integrands $\rho(\sqrt{b^2 + z^2})$.

Usually, integrals like (1.3) are estimated by using the Gaussian functions for both the potential and density distributions. Thus, final expressions are obtained in a certain analytic form (see, for instance, [4],

[5], [6]). But the Gaussian type distributions are only acceptable for light nuclei, whereas for medium and heavy nuclei, one should deal with functions of a greatly extended shape of distributions. To this aim, the Fermi function $u_F(r)$ occurs to be more appropriate, and it is usually applied in numerical calculations. However, if one uses it in analytic estimations, then one encounters serious mathematical and numerical difficulties. Sometimes, one can overcome these difficulties by representing $u_F(r)$ as the sum of Gaussian functions [7]

$$u_F(r,R,a) = \frac{1}{1+\exp[(r-R)/a]} = \sum_{n=1}^{N} c_n \exp\left(-\frac{r^2}{d_n^2}\right), \qquad (1.4)$$

giving for (1.3) the result

$$I_F(b) = \int_{-\infty}^{\infty} \frac{dz}{1+\exp[(\sqrt{b^2+z^2}-R)/a]} = \sum_{n=1}^{N} \sqrt{\pi}\, c_n\, d_n \exp\left(-\frac{b^2}{d_n^2}\right). \qquad (1.5)$$

Here $c_n$, $d_n$ and $N$ are fitted so that the adjusted form of $u_F(r)$ is remained to be close to the initial one within a necessary accuracy. Unfortunately, a fit like that should be performed numerically anew for every new set of the input parameters $R$ and $a$. In another work [8], the following prescription

$$I_F(b) = 2R - 2\pi i a \sum_{p=1,3,5...}^{\infty} \left\{ \frac{b_p^+}{\lambda_p^{(+)}} + \frac{b_p^-}{\lambda_p^{(-)}} \right\}, \qquad (1.6)$$

has been established for (1.3), where $b_p^{\pm} = R \pm i\pi a p$, $(p = 1,3,5...)$ are poles of the function $u_F(b)$, $\lambda_p^{(\pm)} = (b_p^{\pm 2} - b^2)^{1/2}$, and the condition $Im\ \lambda_p^{(\pm)} \geq 0$ should be fulfilled. Keeping several ten terms of the sum in (1.6), it is possible to reconstruct the behavior of $I_F(b)$ in the range of changes of $b$ from 0 to its values slightly greater than the radius $R$. However, at greater values of $b$, it is not possible to get a correct exponential decrease of $I_F(b)$, even when several hundred terms are taken into account.

In the present work, we suggest to use another and very simple analytic expression for the profile integral (1.3) obtained in [9] for realistic distributions described by the symmetrized Fermi function $u_{SF}$. This

expression reconstructs fairly well its exact behavior within the whole range of real $b$ values and keeps the above-mentioned poles at $b = b_p^{\pm}$. On this basis in [10], calculations were done of differential cross sections which well coincide with the results of numerical solutions of the wave equation. In Sec.2, we show that this profile integral and the corresponding eikonal phase $\Phi_N(b)$ can also be successfully used for calculations of the total reaction cross sections. In Sec.3, an obvious model is constructed for analytic calculations of the total reaction cross sections which enables one to distinguish easily between the contributions from internal and peripheral regions of the nucleus-nucleus interaction. Also, we have traced effects of the Coulomb field inclusion on these contributions, as well as on transparency of nuclei. In Sec.4, the origin is pointed out of continuous ambiguity inherent in the optical potential parameters obtained from experimental cross sections, and general conclusions are drawn.

## 2 Eikonal phase for a symmetrized Fermi function and calculations of the total reaction cross sections

The popular Woods-Saxon potential, having an extended spatial distribution, corresponds to behavior of the Fermi function $u_F(r)$ (1.4). But it comes more true to deal with its symmetrized form:

$$u_{SF}(r) = \frac{\sinh(R/a)}{\cosh(R/a) + \cosh(r/a)}, = u_F(r) - \delta(r) \qquad (2.1)$$

where

$$\delta(r) = \frac{\exp(-R/a)}{\exp(r/a) + \exp(-R/a)}. \qquad (2.2)$$

Indeed, starting with calculations of nuclear form factors [11] and [12], this shape has been used frequently instead of $u_F$. At $R \gg a$ when $\delta(r) \ll 1$, they almost completely coincide with one another in the range of $r \geq 0$. It means that they can be employed with the same success for simulation of the matter distribution in medium and heavy nuclei and also used as patterns when constructing the nucleus- nucleus potentials. However, for light nuclei with a very developed surface ($a \simeq R$), these

functions have rather different shapes at $r <\sim R$. Moreover, from the physical point of view, the lack of the Fermi distribution is because of $u_F$ having a nonzero derivative in the center of a nucleus, e.g. $u'_F(0) \neq 0$ while $u'_{SF}(0) = 0$. The same shortage of the Fermi function makes its use difficult in the complex plane when calculating amplitudes of scattering, many troubles arise if one tries to get explicit expressions for several integrals, etc. (see, for instance, [13], [14]). So, namely with the help of the function $u_{SF}$ in [9], a strict enough and explicit expression was found for a profile integral that we are going to use below. Substituting (2.1) into (1.3) we represent the profile integral in a more convenient form by changing variables $\zeta = z/a$, $\beta = b/R$, and $C = R/a$:

$$I(b) \equiv I(\beta R) = 2R\mathcal{I}(\beta), \tag{2.3}$$

$$\mathcal{I}(\beta) = \frac{1}{C}\int_0^\infty \frac{\sinh C \; d\zeta}{\cosh C + \cosh\sqrt{(\beta C)^2 + \zeta^2}} = u_{SF}(\beta)P(\beta, C). \tag{2.4}$$

In this expression, the main dependence on the impact parameter $b$ or $\beta$ is determined by the symmetrized Fermi function

$$u_{SF}(\beta) = \frac{\sinh C}{\cosh C + \cosh \beta C}, \tag{2.5}$$

and the second function $P(\beta, C)$ makes only a small correction to its behavior at fixed $C$. For $P(\beta, C)$, it is possible to obtain a compact expression [9] as

$$P(\beta, C) \simeq P_a(x) = \frac{1}{C}\ln(4/x), \tag{2.6}$$

where

$$x(\beta, C) = \frac{2}{\kappa}\,\frac{1}{1 + \dfrac{\cosh C}{\cosh \beta C}}\left\{1 + \frac{\kappa - 1}{\cosh \beta C}\right\}. \tag{2.7}$$

Here the parameter $\kappa$ is connected with $C$ according to the formula

$$\log \kappa = 0.47909 + 0.15025\; C - 0.001938\; C^2, \tag{2.8}$$

found in [9] by fitting the approximate analytic form of the integral $\mathcal{I}(\beta)$ (the right hand-side of (2.4)) to its magnitudes obtained by numerical

calculations when the parameters $\beta$ and $C$ are displayed in their typical physical limits $0 < \beta < 2$ and $5 \leq C \leq 20$. If one takes into account that for heavy ions the region of the main contribution is concentrated near the nuclear surface $b = R$ or $\beta = 1$, then $x \simeq 1/\kappa$ and for the correcting function we have a simple expression as follows

$$P_a(1, C) \simeq \frac{1}{C} \ln 4\kappa = \frac{1}{C} \left[2.489453 + 0.34597\ C - 0.0046\ C^2\right]. \quad (2.9)$$

It results in the corresponding nuclear phase

$$\Phi_N(b) = -\frac{2RU_0}{\hbar v} \frac{\sinh(R/a)}{\cosh(R/a) + \cosh(b/a)} P_a(1, C). \quad (2.10)$$

Figure 1 exhibits the comparison of the behavior of profile integrals, calculated by numerical integrations of (2.4) and by its analytic representation in the left hand-side of eq.(2.4). It is seen that at different combinations of colliding nuclei, the results are in appropriate agreement with each other when the correcting function $P_a(\beta, C)$ is taken in its analytic form (2.6). A little worse coincidence is for $P_a(1, C)$ approximated by (2.9). Nevertheless, this difference is noticeable only at $b < R$, in the range of strong absorption, and, as it will be seen below, weakly affects the behavior of cross sections. The values of $C = R/a$ pointed in the Figure correspond to geometric parameters of Fermi distributions of Woods-Saxon potentials fitted to the experimental data in [15] and [16].

To check how successful the analytic expressions for nuclear eikonal phases can reproduce the differential cross sections, calculated by the exact numerical solution of the wave equation, we have to do the respective calculations of the elastic scattering amplitude in the framework of the Glauber-Sitenko approach [2], [3]

$$f(q) = ik \int_0^\infty db\ bJ_0(qb)\ (1 - e^{i\Phi_N + i\Phi_C}), \quad q < \sqrt{2k/R}. \quad (2.11)$$

A characteristic feature of nucleus-nucleus scattering is such that the Coulomb interaction plays a significant role. As usual, we utilize an explicit expression of the Coulomb eikonal phase for the potential of the uniformly charged sphere with radius $R_u$:

$$\Phi_{uc}(b) = \begin{cases} 2\eta \left[\ln(kR_u) + \ln(1 + \sqrt{1 - \frac{b^2}{R_u^2}}) - \frac{1}{3}\sqrt{1 - \frac{b^2}{R_u^2}}(4 - \frac{b^2}{R_u^2})\right] & b \leq R_u \\ \Phi_{pc}(b) & b > R_u \end{cases} \quad (2.12)$$

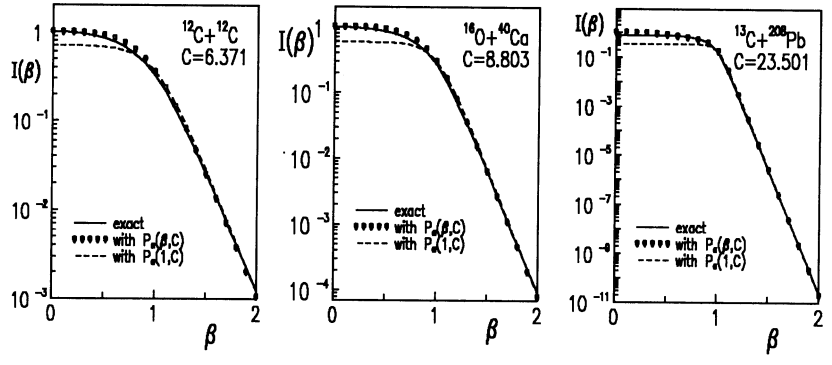


Figure 1: *Comparison of exact (full lines) and approximate profile functions calculated with correcting functions $P_a(\beta, C)$ (2.6) (squares) and P (1,C) (2.9) (dashed lines) for the symmetrized Fermi function.*

Here $\eta = Z_1 Z_2 e^2/\hbar v$ is the Sommerfeld parameter; and $\Phi_{pc}(b) = 2\eta \ln(kb)$, the eikonal scattering phase of a point- like charge. It is seen that, once (2.12) is included into the amplitude (2.11), the problem arises in integrating at large distances because of divergent terms of the form $\exp(2\eta i \ln(kb))$. This difficulty can be removed if in the parentheses under the integral (2.11) one adds and subtracts the eikonal function of the point-like charge $\exp(i\Phi_{pc})$. So, we have

$$f(q) = f_{pc}(q) + ik \int_0^\infty db\ bJ_0(qb)\ e^{i\Phi_{pc}} \left(1 - e^{i\Phi_N + i\delta\Phi_{uc}}\right), \quad (2.13)$$

where the addition $\delta\Phi_{uc} = \Phi_{uc} - \Phi_{pc}$ to the nuclear phase does not comprise the logarithmic term at large $b$, and $\Phi_N(b \to \infty) = 0$. The point-like charge scattering amplitude $f_{pc}(q)$ in (2.13) is known in the explicit form [2]:

$$f_{pc}(q) = -ik \int_0^\infty db\ b^{1+2i\eta} J_0(qb) =$$

$$= -\frac{2k\eta}{q^2}\ e^{-2i\eta \ln(q/2k) + 2i \arg\ \Gamma(1+i\eta)}. \quad (2.14)$$

In this way, the problem is resolved of numerical integration of the scattering amplitude when the Coulomb phase is taken into consideration.

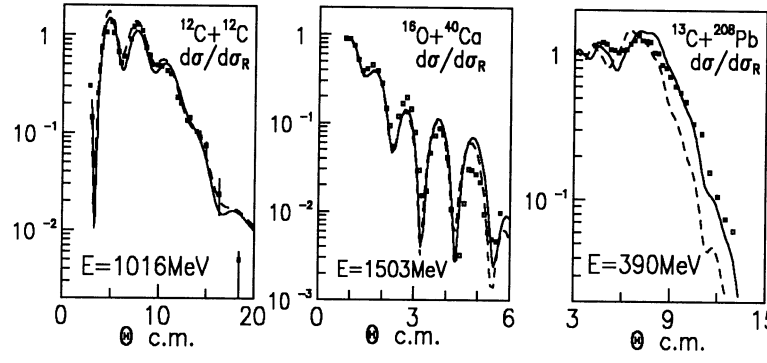


Figure 2: *Differential cross sections of nucleus-nucleus scattering: squares represent experimental data; the calculations with the analytic phases with $P_a(\beta, C)$ are pointed as full lines; and with $P_a(1, C)$, dotted lines for two left figures. In the right picture, the dotted line shows the curve calculated without the Coulomb distortion of the trajectory.*

In scattering of heavy ions, one more modification of the amplitude (2.11) should be made in view of the effects of distortion of the straight line path of integration. Indeed, in the strong long-range Coulomb potential, this effect can be taken into account [17] by adding the classical momentum $q_c = 2k\sin(\theta_c(b)/2)$ to the transfer momentum $q$ where $\theta_c$ is a deflection angle in the Coulomb field. But if one works with the transformed amplitude (2.11), then it is enough to change, in the nuclear eikonal, the impact parameter $b$ in asymptotics by $b_c$ in the range of contact of nuclei, and the probability flux $v$ by $(b/b_c)v$ [18]. The value

$$b_c = \bar{a} + \sqrt{b^2 + \bar{a}^2}, \tag{2.15}$$

where $\bar{a} = \eta/k = (R_c/2)(U_c(R_C)/E)$ is a half-distance of the closest approach in the Coulomb field at $b = 0$, and $U_c = Z_1 Z_2 e^2/R_c$ is the Coulomb potential at the point of the characteristic radius of a charged system.

As an example, Fig.2 shows differential cross sections calculated for scattering of $^{12,13}$C and $^{16}$O on several nuclei at different energies. The experimental data are taken from [15], [16], [19], where the fit of parameters of the Woods-Saxon optical potential was made on the basis of numerical solutions of the wave equation. We used the same parameters in

our calculations with the help of eqs.(2.13)-(2.15) employing the analytic eikonal phases for the symmetrized Woods-Saxon potential. It is seen that the Glauber-Sitenko approach with the analytic phases of eikonals describes well the experimental differential cross sections when one uses both the $P_a(\beta, C)$ (2.6) correction function (full curves for $^{12}C + {}^{12}C$ and $^{16}O + {}^{40}Ca$) and $P_a(1, C)$) and $P_a(1, C)$ (dashed) (2.9). For the case of $^{13}C + {}^{208}Pb$ at $E = 390$ MeV, we give the results (dashed curve) without the Coulomb distortion. One can see that in this case the distortion is very important to be included, while in two other cases at larger energies and lower Coulomb barriers its influence may be practically neglected. As one can expect, the distortion appears in scattering on heavier nuclei and at relatively low energies. In other quoted cases it turned out to be of no importance.

**Table 1.** Comparison of total reaction cross sections in the Glauber-Sitenko approach with the exact calculations performed in [15,16,19].

| Reaction | $E_{lab}$, MeV | $\sigma_R^{appr}$(SF),mb | $\sigma_R^{exact}$(F), mb |
|---|---|---|---|
| $^{16}$O+$^{40}$Ca | 1503 | 1983 | 1996 |
| $^{16}$O+$^{90}$Zr | 1503 | 2711 | 2749 |
| $^{16}$O+$^{208}$Pb | 1503 | 3614 | 3602 |
| $^{13}$C+$^{208}$Pb | 390 | 2868 | 2898 |
| $^{12}$C+$^{12}$C | 1016 | 1093 | 1040 |
| $^{12}$C+$^{12}$C | 360 | 1147 | 1258 |

In Table 1, we report the comparison of exact calculations of total reaction cross sections, performed in [15] and [16] by numerical calculations of the wave equation, and our results obtained according to the formula (1.1) with analytic phases of nuclear eikonals. It should be stressed that the exact calculations were done with the Woods-Saxon potential, and our calculations with its symmetrized form but at the same parameters. Moreover, for light nuclei $^{12}C + {}^{12}C$, these potentials significantly differ. One more difference is that, in exact calculations, results depend both on the real and imaginary parts of an optical potential while in the case of high-energy approximation (1.1) they are formed only by its imaginary part. Nevertheless, the difference in calculations does not exceed

1% of the cross sections for all the cases except for $^{12}C + {}^{12}C$ at 390 MeV, where it equals 9% because of an increased role of the real part of the potential at the relatively low energy $E = 360\ MeV$.

# 3 The model of broken trapezium and the total reaction cross section

In the previous section, we convinced that the eikonal nuclear phase with the profile integral (2.4) in the form of symmetrized Fermi distribution $u_{SF}(b)$ describes fairly well the differential scattering cross sections and total reaction cross sections. The shape of this function is such that, surface of the radius $R$ is singled out, where $u_{SF}(R) \simeq 1/2$ and $u'_{SF}(R) = -1/4a$, so that the decrease of this function occurs in the "layer" of thickness $4a$ from the value $u_{SF}(b < R - 2a) \simeq 1$ to $u_{SF}(b > R + 2a) = 0$. This shape can be simulated by the usual trapezium. For example, this model allows one to calculate (1.1) for the total $\pi A$-reaction cross section [20]). Nevertheless, in the case of heavy ion reactions, this model turns out to be too rough, as it does not take into account a more smooth behavior of the function $u_{SF}$ at $b < R_2 = R - a$ $b > R_3 = R + a$. This shortage is to be improved if, at these points, additional kinks are introduced so that the slopes of sides of relevant sections are determined by the derivatives $u'_{SF}(R_1 < b < R_2) = -1/2a$ and $u'_{SF}(R_3 < b < R_{4(5)}) = -1/2a(-1/3a)$ (see Fig.3) where $R_1 = R - 3a$ and $R_{4(5)} = R + 3a(4a)$. On the basis of this model, we give the necessary formulae and comparisons with exact calculations, as well as the analysis of experimental data.

In expression for the total cross section (1.1), we use the eikonal phase in approximated form (2.10), and effects of the Coulomb distortion of the trajectory are included by changing $b \to b_c(b)$ and $v \to (b/b_c)v \simeq [1 - U_c(R_c)/E]^{1/2}v$, where $b_c$ is defined by formula (2.15). Then, according to (2.15) we have $bdb = (b_c - \bar{a})db_c$ and

$$\sigma_R = 2\pi \int_0^\infty db\, b \left(1 - \tilde{T}(b_c)\right) = 2\pi \int_{2\bar{a}}^\infty db_c\, (b_c - \bar{a}) \left(1 - \tilde{T}(b_c)\right), \quad (3.1)$$

where the transparency function is defined as

$$\tilde{T}(b_c) = e^{-\chi(b_c)} = \left(\tilde{T}_0\right)^{u_{SF}(b_c)}, \qquad \tilde{T}_0 = e^{-\tilde{\chi}_0},$$

$$\tilde{\chi}_0 \simeq \frac{\chi_0}{\sqrt{1 - U_c(R_c)/E}}, \qquad \chi_0 = \frac{4RW_0}{\hbar v} P_a(1, C). \tag{3.2}$$

Now we approximate the function $u_{SF}(b)$ with the help of the broken trapezium $u_{bt}(b)$:

$$u_{bt} = \Theta(R_1 - b) + \sum_{n=2,3,4(5)} u_{bt}^{(n)}(b), \tag{3.3}$$

where every section from the three of them, displayed in a surface, is given as

$$u_{bt}^{(n)} = \left[A_n + \frac{1}{a_n}(R_{k(n)} - b)\right] \Theta(R_n - b)\Theta(b - R_{k(n)}). \tag{3.4}$$

Here

$$A_n = \frac{6 - n - \delta_{n,4}}{4}, \qquad a_n = 4(n - 2 + 2\delta_{n,2})a, \quad n = 2, ...5 \tag{3.5}$$

$$R_p = R + (2p - 5 - \delta_{p,5})a, \; p = 1, ...5; \quad k(n) = n - 1 - \delta_{n,5}, \; n = 2, ...5. \tag{3.6}$$

Substituting (3.3) into (3.2), and then into (3.1), and introducing the width for each section

$$\Delta_n = R_n - R_{k(n)} = (2 + \delta_{n,5})a, \qquad n = 2, ...5, \tag{3.7}$$

after elementary integration we obtain

$$\sigma_R = \pi R_1^2 \left[1 - \frac{2\bar{a}}{R_1}\right]\left(1 - \tilde{T}_0\right) + \sum_{n=2,3,4(5)} \left\{ 2\pi \Delta_n R_{k(n)} C_{k(n)} + \pi \Delta_n^2 - \right.$$

$$- 2\pi \frac{a_n R_{k(n)} C_{k(n)}}{\tilde{\chi}_0} \tilde{T}_0^{A_n - \Delta_n/a_n}. \tag{3.8}$$

$$\left. \cdot \left[1 - \frac{\Delta_n}{R_{k(n)} C_{k(n)}} - \tilde{T}_0^{\Delta_n/a_n} + \frac{a_n}{R_{k(n)} C_{k(n)}} \frac{1}{\tilde{\chi}_0}\left(1 - \tilde{T}_0^{\Delta_n/a_n}\right)\right] \right\},$$

where

$$C_{k(n)} = 1 - \frac{\bar{a}}{R_{k(n)}} = 1 - \frac{1}{2}\frac{R_c}{R_{k(n)}}\frac{U_c(R_C)}{E} \tag{3.9}$$

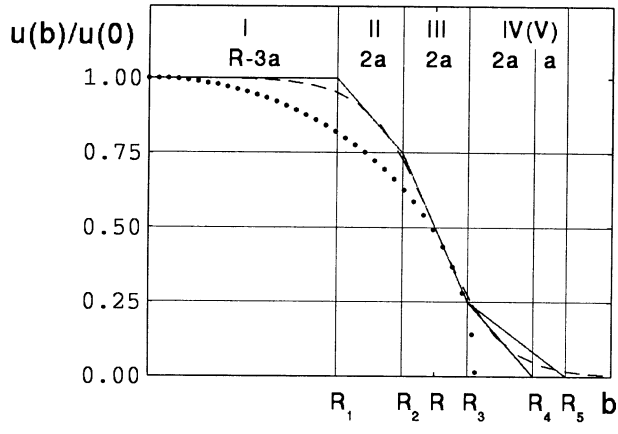


Figure 3: *Symmetrized Fermi function (dotted) with parameters of the radius R and thickness a, and its approximation by the broken trapezium in the surface region (full line). Points show the phase of the square well potential with the equivalent radius* $R_u$.

is a factor that appears side by side with other modifications (3.1) and (3.2) due to the Coulomb distortion. When the Coulomb field is absent, we have $\eta = 0$, $\bar{a} = 0$, and then in (3.8) one should substitute $C_{k(n)} = 1$ and $\tilde{T} \to T_0 = \exp \chi_0$, which gives

$$\sigma_R = \pi R_1^2 (1 - T_0) + \sum_{n=2,3,4(5)} \left\{ 2\pi \Delta_n R_{k(n)} + \pi \Delta_n^2 - \right.$$

$$- 2\pi \frac{a_n R_{k(n)}}{\chi_0} T_0^{A_n - \Delta_n/a_n} \cdot \tag{3.10}$$

$$\left. \cdot \left[ 1 - \frac{\Delta_n}{R_{k(n)}} - T_0^{\Delta_n/a_n} + \frac{a_n}{R_{k(n)}} \frac{1}{\chi_0} \left( 1 - T_0^{\Delta_n/a_n} \right) \right] \right\}.$$

Usually the parameters of potentials in nucleus-nucleus collisions at intermediate energies are such that the quantities $\chi_0 \gg 1$ and $T_0 \ll 1$ (strong absorption in the internuclear region).This enables one to use the following expression for quantitative estimations of the cross section

$$\sigma_R \simeq \pi R_1^2 + \sum_{n=2,3,4(5)} \left( 2\pi \Delta_n R_{k(n)} + \pi \Delta_n^2 \right). \tag{3.11}$$

It is, as it should be expected, the sum of area of the circle with the radius $R_1 = R - 3a$ and areas of the outer ring with the width about $(6 \div 7)a$.

**Table 2.** *Distribution of contributions to cross sections of the* $^{16}O + {}^{A}Z$ *reactions from inner and peripheral regions in different models with the Coulomb distortion and without it. (Definitions of sections I-V are given in Fig.3).*

| target | model | I | II | III | IV (V) | $(R_5, \infty)$ | $\sigma_R, mb$ |
|---|---|---|---|---|---|---|---|
| $^{40}$Ca | SF | 517.7 | 425.5 | 538.4 | 462.5 (494.9) | 59.8 | 2036.3 |
| | SF+C | 517.7 | 425.4 | 533.3 | 382.4 (454.6) | 51.7 | 1982.7 |
| | BT | 517.7 | 425.5 | 537.5 | 407.1 (590.3) | | 2050.9 |
| | BT+C | 517.7 | 425.5 | 531.8 | 465.5 (549.2) | | 2025.3 |
| | U | 517.5 | 424.8 | 528.3 | 13.4 (13.4) | | 1530.7 |
| | U +C | 517.5 | 424.9 | 537.5 | 50.8 (50.8) | | 1484.0 |
| $^{90}$Zr | SF | 568.3 | 500.7 | 657.3 | 707.9 (917.2) | 172.8 | 2816.8 |
| | SF+C | 568.3 | 500.7 | 656.8 | 667.7 (845.1) | 139.9 | 2710.8 |
| | BT | 568.3 | 500.7 | 657.2 | 770.6 (1008.5) | | 2734.7 |
| | BT+C | 568.3 | 500.7 | 656.7 | 749.1 (934.7) | | 2660.4 |
| | U | 568.3 | 500.7 | 656.2 | 96.6 (96.6) | | 1821.8 |
| | U +C | 568.3 | 500.7 | 655.3 | 13.9 (13.8) | | 1738.1 |
| $^{208}$Pb | SF | 1495.2 | 687.2 | 805.7 | 634.2 (765.3) | 95.6 | 3849.0 |
| | SF+C | 1495.2 | 687.2 | 783.9 | 500.9 (587.5) | 60.2 | 3614.1 |
| | BT | 1495.2 | 687.2 | 804.7 | 737.6 (899.6) | | 3886.8 |
| | BT+C | 1495.2 | 687.2 | 784.5 | 634.8 (683.4) | | 3650.3 |
| | U | 1495.0 | 686.1 | 715.9 | | | 2897.0 |
| | U+C | 1495.0 | 685.2 | 513.0 | | | 2693.1 |

In Table 2, we report the total reaction cross section calculations for collisions of the $^{16}O$ projectiles and target nuclei $^{40}Ca$, $^{90}Zr$, $^{208}Pb$. Contributions from different regions of $b$ are singled out in accordance with its values, shown in Fig.3 for the model of broken trapezium. The results are given for three models which describe distributions of the imaginary part of the optical potential: symmetrized Fermi function (SF), broken trapezium (BT), and uniformed distribution (U) with the radius $R_u = R[1 + (7/3)(\pi a/R)^2]^{1/2}$ being equivalent to the SF-form. In all three cases, calculations are shown when the Coulomb distor-

tion was taken into account (+C) and neglected. Kinetic energy of the projectile nucleus $^{16}O$ is $E = 94$ MeV/N, and the parameters $R$ and $a$ are the same as in [19] where the cross sections were calculated by numerical solutions of the wave equation with a Woods-Saxon potential (F-distribution). These cross sections are given in Table 1 and are equal for the mentioned target-nuclei as follows $^{40}Ca$ - 1996 mb, $^{90}Zr$ - 2749 mb, $^{208}Pb$ - 3602 mb. In Table 2, we compare these exact values with calculations in the Glauber-Sitenko approach. One can conclude that the square well model (U-distribution) that is sometimes used for experimental data analyses (see, for instance, [6]), is highly approximate. Indeed, calculations according both to the realistic SF-model and the broken trapezium (BT) show that contributions to the total cross sections, caused by the inner ($b < R$) and outer ($b > R$) interaction regions, are approximately equal. This means that the surface region and its structure play a highly important role in the formation of a total reaction cross section. But the trapezium model, owing to its simplicity, enables us to understand the mechanism of composition of cross sections from selected sections in the range of interaction surface. Then, the Coulomb trajectory distortion reveals mainly itself in the peripheral region, and when this effect is taken into account, the decrease of the cross section by about 20% occurs in the case of heavy target-nucleus $^{208}Pb$ and by 10% at interactions with nuclei of medium atomic weight. It is clear that, as the collision energy decreases, the Coulomb trajectories deflect more far from the region of direct contacts of nuclei, and therefore, the reaction cross sections diminish faster.

# 4 The problem of ambiguity of the potential. Conclusions

One can mention one more advantage of the analytic approach, namely, the possibility to understand the mechanism of revealing the so-called continuous ambiguity in the choice of potential parameters. This is a consequence of the fact that, owing to strong absorption in the inner region, the fit to experimental data mainly depends on the peripheral interaction region [21]. For the first time it was shown with an example of calculations of the cross sections of fast alpha particles scattered on atomic nuclei [22], when instead of the Woods-Saxon potential, a poten-

tial of the exponential form has been chosen as $[U\exp(R/a)]\exp(-r/a)$ that considerably differs from the Woods-Saxon potential inside the inner region and coincides with it at $r \gg R$. Nevertheless, by means of variations of the parameter $a$ and the "strength" $[U\exp(R/a)]$ of the new potential, one could explain some set of data on differential cross sections. Moreover, it is seen that the same value in brackets can be obtained at a continuous set of collections of $R$ and $U$. In Sec. 3, we saw that it was possible to explain experimental data when the primary phase is replaced by a broken trapezium that, in contrast to the exponential form, retains its form inside the inner region whilst the behavior in the peripheral region is approximated by linear forms.

To investigate the origin of the ambiguity in our approach it is not necessary to replace the initial symmetrized Woods-Saxon potential by another, in particular, by approximating it in the peripheral region. The ambiguity mechanism is revealed immediately in the expression for the cross section itself (3.1). To this end, we express this cross section with the help of substitutions $b = \beta R$, $C = R/a$ in the following form:

$$\sigma_R = 2\pi R^2 \left[1 - \frac{U_c(R_c)}{E_{cm}}\right] F(C, D), \tag{4.1}$$

where

$$F(C, D) = \int_0^\infty d\beta\ \beta\ \left[1 - e^{-0.4391\, D\, u_{SF}(\beta, C) P_a(\beta, C)}\right], \tag{4.2}$$

$$D = \sqrt{\frac{A_2}{A_1 + A_2}\frac{1}{\epsilon_{cm}}}\, RW_0, \qquad \epsilon_{cm} = \frac{E_{cm}}{A_1}. \tag{4.3}$$

Here the symmetrized Fermi function $u_{SF}(\beta, C)$ and correcting function $P_a(\beta, C)$ are given by formulae (2.5) and (2.6), respectively. The common parameter of the problem $D$ depends on the combination of such input values as atomic numbers of nuclei $A_1$ and $A_2$, collision energy $\epsilon_{cm}$(MeV) per one nucleon of the projectile nucleus, a depth of the imaginary part of a potential $W_0$(MeV) and the radius $R$(Fermi). The function $F(C, D)$ is to be calculated only once for all the region of available changes of values $C$ and $D$, and then it is used for scanning their values when comparing with experimental data. In Fig.4, as an illustration, the relevant curves $F(C, D)$ are shown in the interval of changes of $D$ from 25 to 350, a step by 25 units, as a function of $C$ in the interval

of $5 \div 20$. As a matter of fact, such curves cover continuously all the surface of the figure.

It is convenient to construct the procedure of selecting parameters of the imaginary part of nuclear potential as follows. An experimental cross section at a given energy should be divided by $2\pi R^2[1 - U_c(R_c)/E_{cm}]$ to obtain $F(C, D)$ and to have the possibility to compare it with the calculated ones in Fig.4. Then, the parameters of radii $R$ and $R_c$ are to be chosen to fix this value. Next, on the $F(C, D)$ plot, a horizontal line should be drawn, and by points of its intersections with the curves one can find the values $C$ and $D$ (continuous set), and according to them one obtains the parameters of diffuseness $a$ and $W_0$. It is interesting to mention that at every given value of radius $R$ there exists a continuous set of parameters $a$, so that all phase curves $\Phi_N(b)$ intersect in the range of the surface at one point $b = R$, and to each of them there corresponds the parameter $W_0$, different from others. As in our approach $a$, $R$ and $W_0$ are the parameters of the potential itself, the ambiguity of phases means indefinite choice of the potential. Then, for example, to the intersection point of phases at $b = R$, there corresponds the point of intersection of the potentials in the region of its diffuseness $r \simeq R\cos^{-1}\theta_c$, where $\theta_c \simeq U_c(R_c)/E_{cm}$. To select the sets of physically important parameters, one can use the known procedures of conservation of a "volume" of the potential and its mean-root squared radius, as well as other physical criteria. All this fitting procedure is to be repeated if, at the beginning, other values of radii $R$ and $R_c$ are chosen. So, we see that the transparency $T(b)$ in fact does not depend on the three parameters $a$, $R$, $W_0$ separately, but on two combinations among them only as $RW_0$ and $C = R/a$. These combinations are, to an extent, the calibration, to be used in the procedure of fitting the cross sections to experimental data narrowing in this way the available sets of parameters.

Summing up, one can conclude that at energies of primary nuclei beginning ¿from 10 MeV/N and more, the Glauber-Sitenko approach is quite acceptable for calculations and analysis of differential cross sections. One can also mention that tested certain form of analytic expression of the profile integral (2.4) for the realistic optical potential with the SF distribution enables us not only to accelerate substantially all computational procedures, but, which is more important, to develop the analytic methods of observable calculations, and, in this way, to analyze

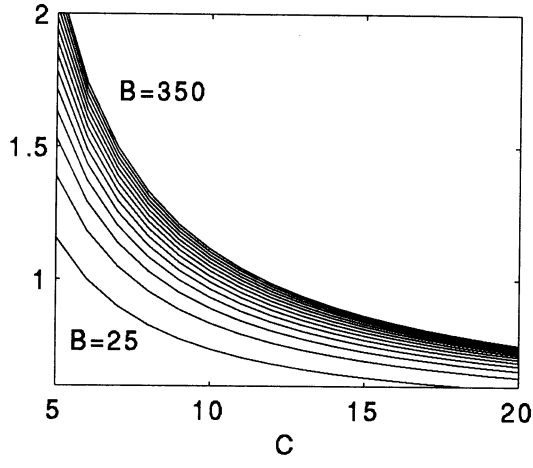


Figure 4: *Plot of continuous ambiguity of fitting parameters $R$, $a$, $W_0$ of the imaginary part of potentials with a shape of symmetrized Fermi function when the reaction cross section depends on their combinations as $C = R/a$ and $D = 4RW_0/\hbar v$.*

the mechanism of cross section formation, as well as to study their obvious form of the dependence of potential parameters, etc. Moreover, dealing with explicit expressions for amplitudes and cross sections one can simply take into account the influence of the Coulomb distortion on final results of calculations. For this purpose, the formal renormalization of the impact parameter should be done. At the same time, the initial scheme of high-energy approximation does not change. Furthermore, in all the cases of calculations, both for differential cross sections of elastic scattering and the total reaction cross sections, we have convinced ourselves that our analytic approximations for eikonal phases give the good coincidence with the results of numerical solutions of the Schroedinger equation at the same potentials of interaction.

This work is carried out under the "Infeld-Bogoliubov Program". V.K.L. thanks the Support of the Leading Scientific Schools under Russian Foundation for Basic Research (RFBR) (grant 00-15-96737) and the Ministry of Education of Russia Foundation (grant 97-40-1.6-6). E.V.Z. is grateful to the RFBR (grant 0001-006-17).

## References


[1] J.-S.Wan a.o., *Transmutation of radioactive waste by means of relativistic heavy ions*, Kerntechnik, v.63, 1998, pp.167-177;

[2] R.J.Glauber, *in* Lectures on Theor. Phys., **1** (Interscience, New York, 1959);

[3] A.G.Sitenko, Ukr.Fiz.J., **4** (1957) 152;

[4] P.J.Karol, Phys.Rev. C, **11** (1975) 1203;

[5] S.Charagi and G.Gupta, Phys.Rev. C, **41** (1990) 1610;

[6] A.Abdul-Magd and A.Talib Ali-Alhinai, Nuovo Cimento A, **110** (1997) 1281;

[7] O.D.Dalkarov and V.A.Karmanov, Nucl.Phys., **A445**, (1985) 579;

[8] J.R.Shepard and E.Rost, Phys.Rev. C, **25** (1982) 2660;

[9] V.K.Lukyanov, E.V. Zemlyanaya, J.Phys.G: Nucl.and Part.Phys., **26** (2000) 357; Preprint JINR, E4-99-260, Dubna, 1999;

[10] V.K.Lukyanov, E.V. Zemlyanaya, A.V.Embulaev, JINR Preprint E4-99-291, Dubna, 1999;

[11] Yu.N.Eldyshev, V.K.Lukyanov, Yu.S.Pol', Yad.Fiz., **16** (1972) 506;

[12] V.V.Burov, Yu.N.Eldyshev, V.K.Lukyanov, Yu.S.Pol', Preprint E4-8029 (1974), JINR, Dubna;

[13] M.Grypeos, C.Koutroulos, V.Lukyanov, A.Shebeko, J.Phys.G: Nucl. and Part.Phys., **24** (1998) 1913;

[14] D.W.L.Sprung, J.Martorell, J.Phys.A: Math.Gen., **30** (1997) 6525;

[15] M.Buenerd et al, Nucl.Phys., **A424** (1984) 313;

[16] J.Y.Hostachy et al., Phys.Let. B, **184**, no.2,3 (1987) 139;

[17] V.K.Lukyanov, Phys.Atomic Nucl. (transl. from russ. Yad.Fiz.), **58** (1995) 1848;

[18] A.Vitturi and F.Zardi, Phys.Rev. C, **38** (1988) 2086.

[19] P.Rossel-Chomaz et al, Nucl. Phys., **A477** (1988) 345.

[20] B.Slowinski, Sov.J.Nucl.Phys., **19** (1974) 301.

[21] G.D.Satchler, *Direct nuclear reactions*, Clarendon, Oxford, 1983.

[22] G.Igo, Phys.Rev., **115** (1959) 1665.



Received by Publishing Department
on May 18, 2000.

Лукьянов В.К., Словинский Б., Земляная Е.В. Е4-2000-103

О роли ядерной поверхности в формировании полного сечения ядро-ядерных реакций

В подходе Глаубера–Ситенко разработана схема расчета ядро-ядерных сечений при промежуточных энергиях с использованием аналитической эйкональной фазы для симметризованного потенциала Вудса–Саксона. Полученные на этой основе дифференциальные и полные сечения хорошо совпадают с результатами численных решений волнового уравнения. Построена наглядная модель фазы, что позволяет разделить в полных сечениях реакций вклады от внутренней и периферической областей взаимодействия. Установлена важная роль ядерной поверхности в формировании сечений реакции, изучено влияние на них кулоновского поля. Выявлена природа неоднозначности оптических потенциалов, получаемых при интерпретации экспериментальных сечений.

Работа выполнена в Лаборатории теоретической физики им. Н.Н.Боголюбова и Лаборатории вычислительной техники и автоматизации ОИЯИ.

Препринт Объединенного института ядерных исследований. Дубна, 2000

Lukyanov V.K., Słowinski B., Zemlyanaya E.V. E4-2000-103

On the Role of Nuclear Surface in Heavy Ion Reaction Cross Section Formation

The Glauber–Sitenko approach is developed for calculations of the nucleus-nucleus cross sections at intermediate energies on the basis of the analytic expression of the eikonal phase for the symmetrized Woods–Saxon potential. Calculations show that the differential elastic and total reaction cross sections occur in a good agreement with those obtained by numerical solutions of the wave equation. For the total reaction cross section, an instructive model of the phase is suggested that allows one to separate contributions from internal and peripheral regions of interaction. An important role of the surface is established in formation of the total cross section, and effects of the Coulomb field are studied, too. The nature of the continuous ambiguity of optical potentials is ascertained for interpreting experimental data.

The investigation has been performed at the Bogoliubov Laboratory of Theoretical Physics and at the Laboratory of Computing Techniques and Automation, JINR.

Preprint of the Joint Institute for Nuclear Research. Dubna, 2000

Макет Т.Е.Попеко

Подписано в печать 26.05.2000
Формат 60 × 90/16. Офсетная печать. Уч.-изд. листов 1,6
Тираж 360. Заказ 52046. Цена 1 р. 90 к.

Издательский отдел Объединенного института ядерных исследований
Дубна Московской области